CHAPTER 9

WAVE KINEMATICS COMPUTATIONS USING BOUSSINESQ MODELS

J. Bosboom[1,2], G. Klopman[1,2], J.A. Roelvink[1,2], J.A. Battjes[1]

ABSTRACT

Existing Boussinesq models are extended to include the computation of the vertical structure of the horizontal velocity. A time-domain model is tested against laboratory measurements of the vertical profile of the horizontal velocity in regular waves; good results are obtained, especially in the near-bed zone. A spectral model, which includes a dissipation formulation to account for wave breaking, is tested against laboratory measurements of bottom velocities in (partially) breaking irregular waves. For moderately long waves, the comparison on velocity variance and skewness, which are relevant to sediment transport, yields good results.

1. INTRODUCTION

The development of numerical models capable of reproducing the hydrodynamics field in the shoaling region and the surf zone is of particular interest to coastal morphological problems. From an evaluation of sediment transport formulations (Bailard, 1981; Roelvink and Stive, 1989), it appears that the third and fourth order oscillatory velocity moments ($<u^3>$ and $<|u|^3u>$ respectively), are the most important parameters in determining the magnitude of the wave-induced sediment transport. These moments are non-zero only for asymmetric (non-linear) motions such as occur in shallow water. Boussinesq equations, describing (weakly) non-linear, relatively long waves propagating in water of varying depth, are suitable for the description of these asymmetries.

Many different forms of Boussinesq equations exist, which differ in frequency-dispersion and shoaling characteristics. Efforts have recently been spent on

1) Netherlands Centre for Coastal Research (NCK), Department of Civil Engineering, Delft University of Technology, PO Box 5048, 2600 GA Delft, The Netherlands
2) DELFT HYDRAULICS, PO Box 177, 2600 MH Delft, The Netherlands

improving the linear frequency dispersion with respect to the conventional Boussinesq equations. Reference is made to Witting (1984), Madsen at al. (1991), Madsen and Sørensen (1992), Nwogu (1993), Dingemans (1994b) and Schröter (1995).

On the basis of these time-domain formulations, frequency-domain formulations have been developed leading to coupled evolution equations for slowly-varying complex Fourier amplitudes. Applications and verifications of spectral evolution equations valid for a mildly sloping bottom and non-breaking waves (Freilich and Guza, 1984) were reported in numerous papers (Elgar and Guza, 1985, 1986; Elgar et al., 1990; Freilich et al., 1990). Spectral evolution equations with improved frequency dispersion were presented by Madsen and Sørensen (1993). They concluded that the agreement between the evolution equations and the time-domain counterpart is most satisfactory, except for the peak values of the highest waves which are underestimated by the spectral evolution equations.

Attempts have also been made to include a formulation for wave breaking in Boussinesq equations to extend their applicability to the surf zone. The concept of surface rollers (Deigaard, 1989) was incorporated in conventional time-domain Boussinesq equations by Schäffer et al. (1993). Eldeberky and Battjes (1996) supplemented the spectral evolution equations of Madsen and Sørensen (1993) with a spectral breaking term which accounts for the energy dissipation due to wave breaking (see, also, Battjes et al., 1993).

Only few efforts have been spent on testing Boussinesq models against velocity data. Verification of conventional Boussinesq models (Brocchini et al., 1992 and Quinn et al., 1994) with a description of the breaking process according to Schäffer et al. (1993) against velocity data for waves breaking partially on a gently sloping beach showed fairly good agreement with measured vertical profiles, especially in the near-bed zone. Elgar et al. (1990) obtained accurate estimates of the velocity variance and skewness in the shoaling region using the model of Freilich and Guza (1984).

The purpose of this paper is to verify the Boussinesq modelling of horizontal velocities under (breaking) waves, especially in the near-bed zone. We use a time-domain model (Dingemans, 1994a) for non-breaking waves and a spectral Boussinesq model (Elderberky and Battjes, 1996) assuming a parabolic expression for the calculation of the vertical structure of the horizontal particle velocities, as is consistent with the Boussinesq approximation.

2. TIME-DOMAIN MODEL

The time-domain equations with improved frequency-dispersion and good shoaling behaviour (Dingemans, 1994a) read in one horizontal dimension:

$$\frac{\partial \zeta}{\partial t} + \frac{\partial}{\partial x}[(h+\zeta)\bar{u}] = 0 \tag{1a}$$

$$\frac{\partial \bar{u}}{\partial t} + \bar{u}\frac{\partial \bar{u}}{\partial x} + g\frac{\partial \zeta}{\partial x} = h\frac{\partial}{\partial t}\left[(\frac{1}{2}+b)\frac{\partial^2(h\bar{u})}{\partial x^2} - \frac{1}{6}h\frac{\partial^2 \bar{u}}{\partial x^2}\right] + bgh\frac{\partial^2}{\partial x^2}\left[h\frac{\partial \zeta}{\partial x}\right] \tag{1b}$$

where b is a fitting parameter for obtaining the best agreement with the frequency dispersion according to Stokes' first order theory. For $b = 1/15$ the phase celerity errors are minimized over the whole range of kh (see Madsen and Sørensen, 1992 and Dingemans, 1994b).

Solution of Eqs. (1) yields values for the surface elevation and the computational (depth-averaged) horizontal velocity. The vertical structure of the horizontal velocity is related to the computational velocity through a parabolic expression depending on the vertical coordinate (Dingemans, 1994b):

$$u(x,z,t) = \bar{u} - \left[\frac{1}{2}h+z\right](h\bar{u})_{xx} + \left[\frac{1}{6}h^2 - \frac{1}{2}z^2\right]\bar{u}_{xx} \tag{2}$$

where $z = 0$ corresponds to the undisturbed position of the free surface.

The numerical integration is based on the scheme as applied by Beji and Battjes (1994), which is essentially based on the formulation by Peregrine (1967). The finite difference equations, in which central difference formulations are used both for time and space derivatives, are solved by using a predictor-corrector method.

The extension to reconstruct the horizontal velocity profile is implemented by discretizing the second-order derivatives in the parabolic expression (2) using central differences in space. A low-pass filter is applied to the values of $\bar{u}$ to obtain stable estimates of the second-order derivative $\bar{u}_{xx}$ and $(h\bar{u})_{xx}$.

3. VERIFICATION OF THE TIME-DOMAIN MODEL

Experimental data

The model described above was verified against laboratory measurements of non-breaking monochromatic waves performed by Luth et al. (1994) in a wave flume with a submerged trapezoidal bar (see Fig. 1) as part of the EU-sponsored Large Installations Plan. The flume was 45 m long, 1 m wide and had a still water depth of 80 cm on each side of the bar. The incident wave conditions are T =

1.50 s and H = 0.06 m. Velocity measurements were carried out at different points in the vertical at 15.50 m and 21.72 m from the wave maker using two 3-beam, 2-component Laser Doppler Velocitymeters.

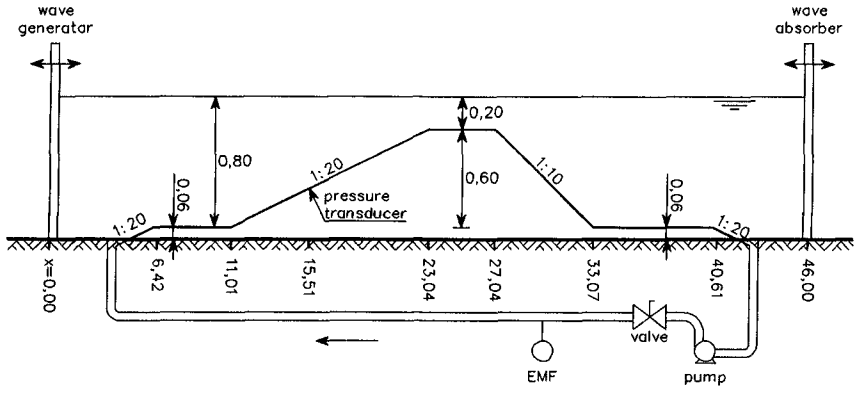

Fig 1 Experimental set-up, all dimensions in m, from Luth et al (1994)

Computational parameters

The time and spatial steps used in the computation were approximately equal to 1/150 of the incident wave period and wave length, respectively. At the seaward boundary, the Courant number $c(\Delta t/\Delta x)$ was approximately one.

Discussion of results

Fig. 2 shows for both stations time-domain comparisons of the measured and computed bottom velocity as well as the velocity evaluated at a level close to where the depth-averaged velocity may be found ($z \approx -0.4\ h$). For the measured bottom velocity in Fig. 2, the value at approximately 2 cm from the bed, just outside the boundary layer, was taken. The time-window in Fig. 2 was chosen in such a way that permanent wave profiles are obtained in the computations. Fig. 3 gives the vertical profiles of the horizontal velocity profile for two different wave phases, corresponding to a crest and a trough in the computations.

Fig. 2 shows that the asymmetry about the horizontal axis occurring on the seaward slope is well represented. The depth-averaged velocity at the crest is slightly overestimated by the Boussinesq model, while the agreement is very good for the trough values. It was found that the surface elevation exhibits a similar overestimation of the crest values. The bottom velocities are predicted quite well, with a small overestimation of the trough values by the model.

Fig. 3 shows a fair agreement between the measured and computed velocity profiles, especially for the lower half of the profile. A small but systematic overestimation of the velocity is found, which is particularly evident for the crest values near the surface.

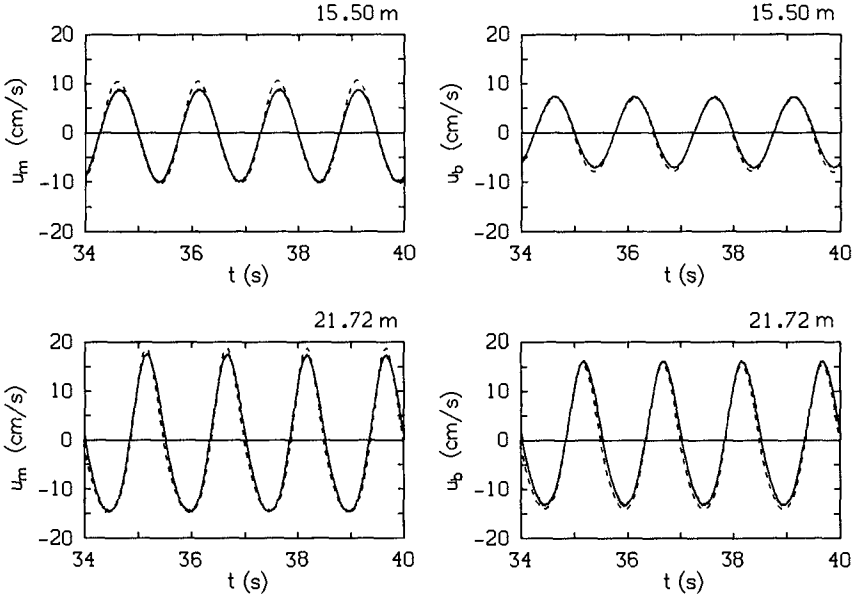

Fig. 2 Measured (solid line) and computed (dotted line) horizontal velocity u_m, evaluated at a level close to where the depth-averaged velocity may be found (top), and near-bed velocity u_b, evaluated at approximately 2 cm from the bed (bottom), for x = 15.50 and 21.72 m respectively.

4. FREQUENCY DOMAIN MODEL

Assuming slowly-varying complex Fourier amplitudes and uni-directional wave propagation, evolution equations for the complex amplitudes were derived by Madsen and Sørensen (1993) and extended by Eldeberky and Battjes (1996) with a formulation for dissipation of energy due to breaking which reduces the spectral amplitudes in the same proportion without affecting the spectral shape. Starting point of the derivation of the spectral evolution equations were time-domain Boussinesq equations (Madsen and Sørensen, 1992) valid for a slowly-varying bottom ($|\mathrm{d}h/\mathrm{d}x| \ll kh$).

Madsen and Sørensen (1993) formulated solutions for the free-surface elevation in terms of Fourier series with spatially varying coefficients:

$$\zeta(x,t) = \sum_{p=-\infty}^{\infty} A_p(x) \exp[i(\omega_p t - \psi_p(x))] \ , \tag{3}$$

where p indicates the rank of the harmonic, A_p is the complex Fourier amplitude, ω_p is the angular frequency and $\mathrm{d}\psi_p/\mathrm{d}x = k_p(x)$ is the wave number in the linear

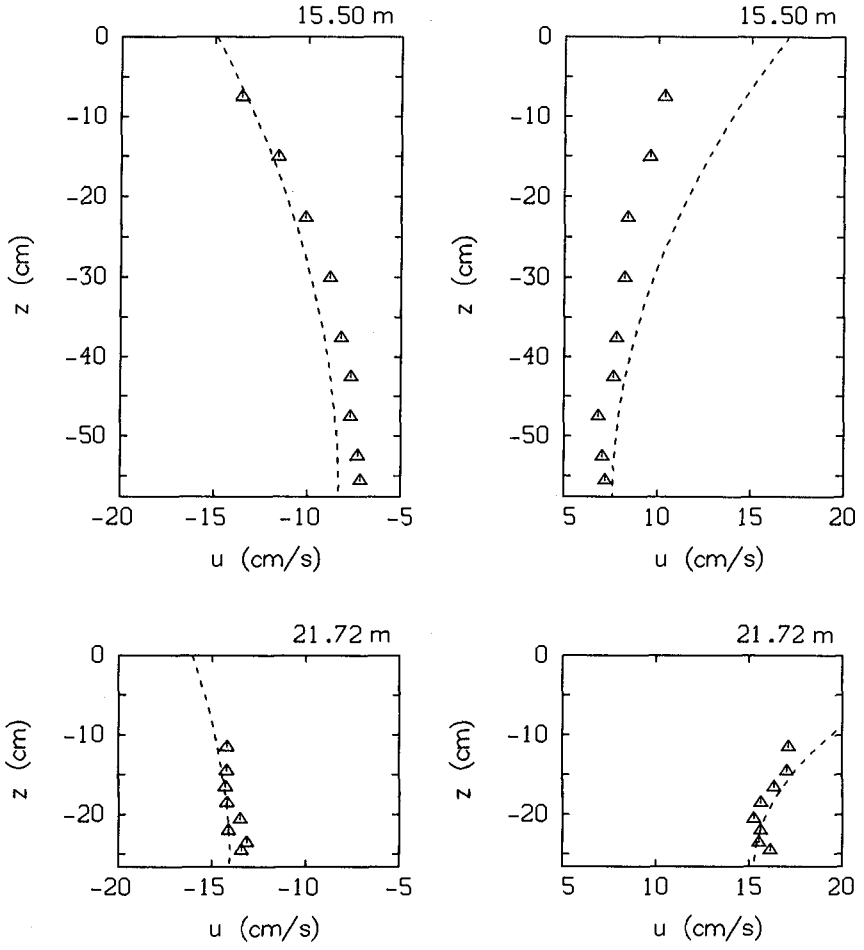

Fig. 3 Comparison of measured (triangles) and computed (dotted line) horizontal velocity vertical profile at x = 15.50 m and 21.72 m respectively, for two different wave phases corresponding to a trough (left) and a crest (right)

approximation. Note that $\omega_{-p} = -\omega_p$, $\psi_{-p} = -\psi_p$, $A_{-p} = A_p^*$ with '*' denoting the complex conjugate. The frequencies are determined by $\omega_p = p\Delta\omega$ where $\Delta\omega$ is the lowest frequency of interest. The wave number k_p can be determined from the linear dispersion relation of the equations.

The evolution equations read, with p covering the interval from $p = 1$ to ∞,

$$\frac{dA_p}{dx} = -\beta_5 \frac{h_x}{h} A_p - i2g\,(F_p^+ + F_p^-) - \tfrac{1}{2}\frac{D}{F} A_p \,, \tag{4}$$

where the first term in the right-hand side of Eqs. (4) represents linear shoaling, the second and the third term represent the triad sum and difference interactions respectively and the last term is the dissipation term representing the contribution due to wave breaking. Here F is the total local rate of energy flux per unit width and D is the total local rate of random-wave energy dissipation per unit area due to breaking. Expressions for the terms F_p^+ and F_p^- and the shoaling coefficient β_5 can be found in Madsen and Sørensen (1993). The energy dissipation rate D can be computed using the energy dissipation model of Battjes and Janssen (1978) or comparable methods (e.g. Thornton and Guza, 1983); here we use the model of Battjes and Janssen (1978).

In the linear approximation, the depth-averaged velocity is expressed in terms of surface elevation using the lowest-order approximation for the volume flux q in a progressive wave:

$$\bar{u}(x,t) \approx \frac{q}{h} \approx \sum_{p=-\infty}^{\infty} \frac{\omega_p}{k_p h} A_p(x) \exp[i(\omega_p t - \psi_p(x))] \,. \tag{5}$$

Note that in this way only the purely oscillating part of the horizontal velocity is predicted by the model; the time-averaged component of the velocity is eliminated upon linearization.

In order to compute the horizontal velocity profile as a function of the depth, we use the parabolic profile for the constant depth situation (Eq. 2 with h-derivatives omitted). Substituting Eq. (5) while neglecting all x-derivatives of A_p, k_p and h, yields the following expression for the horizontal velocity profile in terms of Fourier series:

$$u(x,z,t) = \sum_{p=-\infty}^{\infty} \frac{\omega_p}{k_p h} A_p(x,z) \left[1 + k_p^2 \left[\frac{1}{3}h^2 + zh + \frac{1}{2}z^2\right]\right] \exp[i(\omega_p t - \psi_p(x))]. \tag{6}$$

The evolution equations which are first-order ordinary differential equations are numerically integrated using a fourth-order Runge-Kutta method. The upwave boundary condition for the integration is a set of complex amplitudes A_p (p = 1,2,3...P).

5. VERIFICATION OF THE FREQUENCY DOMAIN MODEL

Experimental data

The prediction of horizontal velocities and velocity moments was verified against wave channel measurements of irregular (partially) breaking waves propagating over a concave sandy beach. The experiments were carried out within the framework of the EU-sponsored Large Installations plan (Arcilla et al., 1993; Roelvink and Reniers, 1995). Two different experimental data sets (i.e. test 1a and 1c) were used. The incident peak period T_p and significant wave height H_{m0} are T_p = 4.9 s and H_{m0} = 0.9 m and T_p = 8.0 s and H_{m0} = 0.6 m for tests 1a and 1c respectively. In the experiments the low frequency energy is kept at a reasonable level by an active wave absorption system at the wave-maker. Surface elevations and velocities were measured at several locations along the wave channel. The velocity measurements were carried out at several distances from the bed. Since the spectral model only predicts the purely oscillating part of the velocity the time-averaged velocity component was filtered from the measured signals.

In experiment 1a the wave breaking is strong. The monotonic sandy beach profile (Fig. 4) allows for wave breaking to take place over a large distance; the experiments showed a gradual decrease of the significant wave height at distances from 100 m up to about 140 m from the wave board, beyond which the wave breaking gets strong. In experiment 1c on the contrary, a barred beach profile is present (Fig. 5). The wave breaking is mild and is concentrated behind the bar, the crest of which is located around 138 m.

The upwave boundary conditions used in the numerical computations are obtained from the measured surface elevations at 20 m by the use of a standard FFT algorithm.

Computational parameters

Besides the bottom geometry and the upwave boundary, the model input comprises the breaking coefficient $\gamma = H_m/h$ in which H_m is the maximum wave height, the bandwidth Δf, the number of frequency components P and the spatial step Δx. The spatial step was chosen Δx = 0.5 m and the breaking coefficient γ = 0.85 in accordance with the γ-value used by Eldeberky and Battjes (1996). A cut-off frequency of 1 Hz was used in the simulations. The length of the simulated time record was T = 2048 s for both experiments, resulting in a number of frequency components P = 2048 and a bandwidth $\Delta f = 4.883*10^{-4}$ Hz.

Analysis of time-series

The comparison between measurements and computations was carried out on amongst others velocity variance and third order velocity moments, the latter being the most important variable in determining the magnitude of the net bedload transport rate. In computing the variance and third order moment of the

bottom velocity it was assumed that the total oscillatory velocity signal u consists of a short wave averaged low-frequency component u_{lo} and a short wave component u_{hi}. The lowest short wave frequency was set to half the peak frequency.

Assuming u_{lo} and u_{hi} to be uncorrelated, the velocity variance is given by:

$$<u^2> = <u_{hi}^2> + <u_{lo}^2> , \tag{7a}$$

where the $< >$ indicate time-averaging over the short wave and wave group scale.

Assuming in addition that $u_{lo} \ll u_{hi}$, Roelvink and Stive (1989) demonstrated that the most important contributions of the oscillatory part of the velocity to the third order velocity moment are given by:

$$<u^3> = <u_{hi}^2 u_{hi}> + 3<u_{hi}^2 u_{lo}> + \ldots . \tag{7b}$$

The first term in the right-hand side of Eq. (7b) is related to the short wave asymmetry, whereas the second term is associated with the interaction between the long wave velocity and the slowly-varying short wave velocity variance.

For both the measured and the computed bottom velocity time series, the three terms in Eqs. (7a-b) were separately calculated and plotted.

Discussion of results

Fig. 4 shows that, except for the last station behind the bar, the short wave velocity variance is very well predicted, indicating that the spectral energy density for the higher frequencies is well reproduced by the model. The model slightly underestimates the total velocity variance for the stations closest to the bar. This can be seen to originate from the inaccurate reproduction of the long wave velocity variance for these stations. This may be the result of a standing low-frequency wave pattern present in the channel with a node in the low-frequency surface elevation and hence large velocity amplitudes around station 5, which are not reproduced by the model because of the assumption of uni-directional wave propagation. Another possible cause could be a too strong reduction of the low frequency energy by the wave breaking formulation.

The third order velocity moment, which can be seen to be dominated by the short wave asymmetry, is largely underestimated by the model. This appeared to be a result of an underestimation of the peak values of the highest waves, which was already reported by Madsen and Sørensen (1993). The agreement is reasonable for the last two stations where strong wave breaking occurs. The long wave contribution is predicted rather well. Increasing the maximum frequency and the frequency resolution did not improve the numerical results.

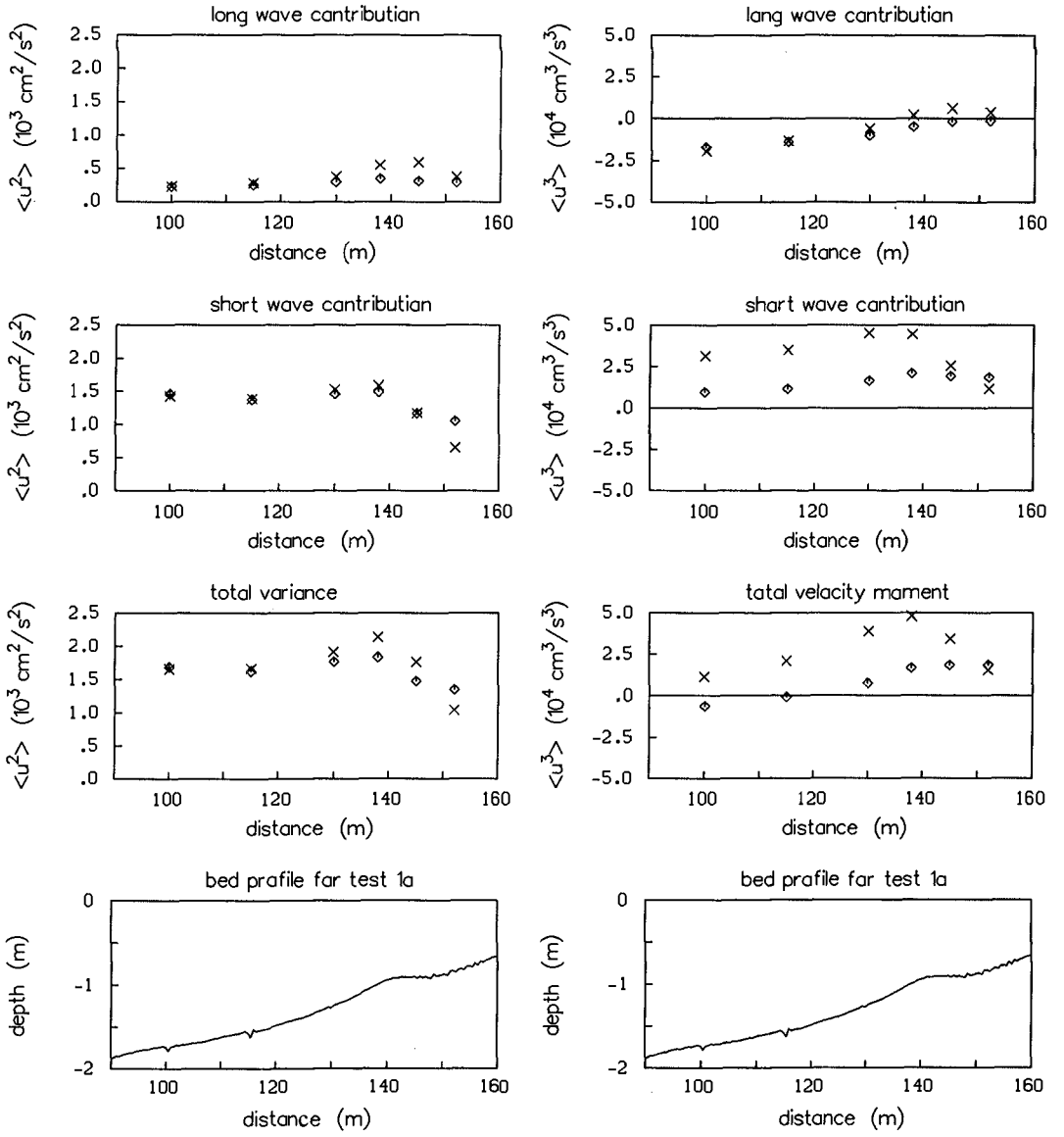

Fig. 4 Comparison of measured (crosses) and computed (diamonds) bottom velocity variance (left) and third order moments (right): long wave contribution, short wave contribution and total moment respectively; experiment 1a. Reprinted from J. Coastal Eng., Bosboom et al., 1996, with kind permission from Elsevier Science-NL, Amsterdam, The Netherlands.

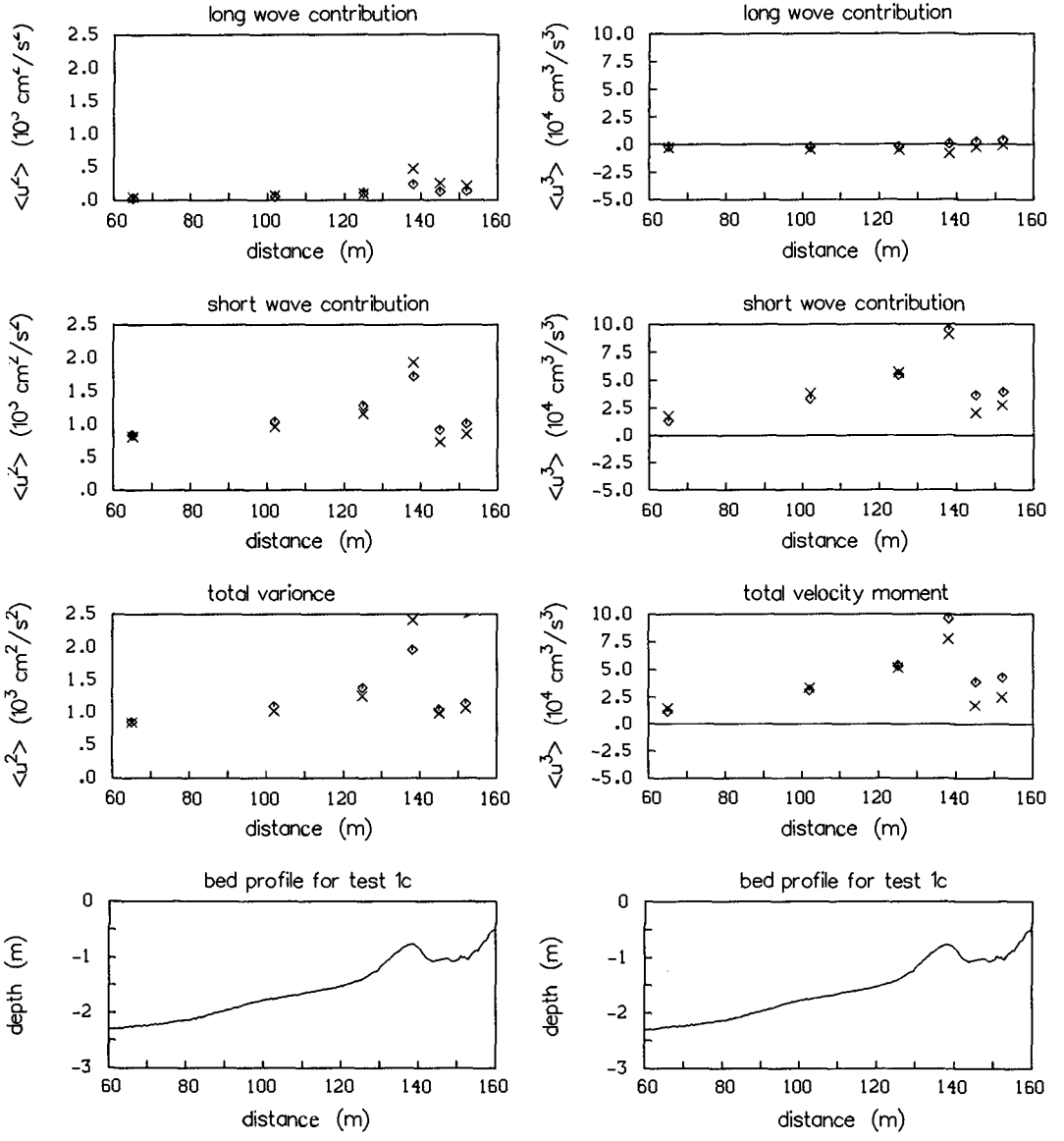

Fig. 5 Comparison of measured (crosses) and computed (diamonds) bottom velocity variance (left) and third order moments (right): long wave contribution, short wave contribution and total moment respectively; experiment 1c. Reprinted from J. Coastal Eng., Bosboom et al., 1996, with kind permission from Elsevier Science-NL, Amsterdam, The Netherlands.

Test 1c shows an encouraging agreement between measured and predicted variance and third order moments (Fig. 5), especially up to the bar crest. The underestimation of the peak values was found to be less significant than for test 1a. The less good agreement beyond the bar crest, also found by Eldeberky and Battjes (1996) for surface elevation spectra, can possibly be ascribed to the relatively steep bottom beyond the bar crest ($|h_x|/kh = 0.52$ for the primary wave) which is in contrast with the assumption of slowly-varying bottom ($|h_x|/kh \ll 1$).

The velocity variance in test 1c (Fig. 5) is predicted well. The difference between the total velocity variance determined from the computed and measured time series at the bar crest is for the larger part the result of the incorrect representation of the long wave energy. As for test 1a, this is can possibly be ascribed to a standing wave pattern in the wave channel or to a too strong reduction of low-frequency energy by the breaking formulation.

It can be concluded that for test 1c the third order velocity moments compare very well with the measurements. For test 1a as well as 1c, the short wave energy is predicted well by the model. The underprediction of the short wave asymmetry by the model in test 1a is therefore the result of an incorrect representation of the phases of the harmonic components. This might be partly due to the larger degree of non-linearity as compared to test 1c, such that the wave breaking already occurs at 100 m from the wave board and continues for a large propagation distance. Besides, the peak period is smaller in test 1a which decreases the accuracy of the frequency dispersion as well as the validity of the assumption of slowly-varying complex amplitudes underlying the evolution equations.

6. CONCLUSIONS

The modelling of horizontal velocities in non-breaking and breaking waves on a beach using Boussinesq-type models has been studied. Time-domain simulations of regular waves indicate that the use of a parabolic vertical distibution of the horizontal particle velocity yields realistic predictions, especially in the near-bed zone.

Horizontal velocities in the near-bed zone in (partially) breaking random waves have been simulated using a frequency-domain Boussinesq model. A fair prediction of the velocity variance was found. For the test with the longer wave period, the third order velocity moments are predicted well by the model. The shorter wave test however, shows an underestimation of the velocity moments due to an underestimation of the crest values of the highest waves. This was seen to be the result of an inaccurate representation of the phases of the higher harmonics.
Further research is necessary to determine whether the discrepancies result from the water-depth restrictions of the Boussinesq equations or from additional assumptions made in the derivation of the evolution equations. Further, attention

should be paid to the inclusion of higher-order derivatives in the spectral evolution equations and the mean velocity in the velocity computation.

ACKNOWLEDGEMENTS

This work was undertaken as part of the MAST-2 G8 Coastal Morphodynamics Research Programme. It was funded jointly by Delft Hydraulics, Delft University of Technology and the Commission of the European Communities, Directorate General for Science, Research and Development under contract no. MAS2-CT92-0027. The laboratory data used were obtained during experiments in the framework of the "Access to Large-scale Facilities and Installations Programme" (LIP), which were funded by the Commission of the European Communities, Directorate General for Science, Research and Development under contract no. GE1*-CT91-0032 (HSMU).

REFERENCES

Arcilla, A.S-, J.A. Roelvink, B.A. O'Connor, A. Reniers and J.A. Jimenez, 1994. The Delta Flume '93 Experiment. *Proc. Coastal Dynamics Conf.*, UPC, Barcelona, Feb. 1994: 488-502.

Bailard, J.A., 1981. An energetics total load sediment transport model for a plane sloping beach. *J. Geophys. Res., 86(C11)*: 10938-10954.

Battjes, J.A. and J.P.F.M. Janssen, 1978. Energy loss and set-up due to breaking of random waves. *Proc. 16th Int. Conf. Coastal Eng*: 569-587. ASCE, New York.

Battjes, J.A., Y. Eldeberky and Y.S. Won, 1993. Spectral Boussinesq modelling of breaking waves. In *Ocean Wave Measurement and Analysis*, edited by O.T. Magoon and J.M. Hemsley. ASCE, New York, pp. 813-820.

Beji, S. and J.A. Battjes, 1994. Numerical simulation of nonlinear wave propagation over a bar. *Coastal Eng., 23*: 1-16.

Bosboom, J., G. Klopman, J.A. Roelvink and J.A. Battjes, 1996. Boussinesq modelling of wave-induced horizontal particle velocities. *Coastal Eng.*, submitted for publication.

Brocchini, M., M. Drago and L. Iovenitti, 1992. The modelling of short waves in shallow waters. Comparison of numerical methods based on Boussinesq and Serre equations. *Proc. 23rd Int. Conf. Coastal Eng.*, ASCE, New York, 4: 76-88.

Deigaard, R., 1989. Mathematical modelling of Waves in the Surf Zone. Prog. Report 69, ISVA, *Technical University of Denmark*, Lyngby, pp. 47-59.

Dingemans, M.W., 1994a. Comparison of computations with Boussinesq-like models and laboratory measurements. *Mast-G8M Note*, Project 1, 30 pp.

Dingemans, M.W., 1994b. Water Wave Propagation Over Uneven Bottoms. *Ph.D. Thesis, Delft University of Technology*, November 1994, 780 pp. Extended version to be published by World Scientific, Singapore, 1996.

Eldeberky, Y. and J.A. Battjes, 1996. Spectral modelling of wave breaking:

Application to Boussinesq equations. *J. Geophys. Res., 101(C1)*: 1253-1264.

Elgar, S. and R.T. Guza, 1985. Shoaling gravity waves: comparisons between field observations, linear theory, and a non-linear model. *J. Fluid Mech., 158*: 47-70.

Elgar, S. and R.T. Guza, 1986. Non-linear model predictions of bispectra of shoaling surface gravity waves. *J. Fluid Mech., 167*: 1-18.

Elgar, S., M.H. Freilich and R.T. Guza, 1990. Model-data comparisons of moments of non-breaking shoaling surface gravity waves. *J. Geophys. Res., 95*: 16,055-16,065.

Freilich, M.H. and R.T. Guza, 1984. Nonlinear effects on shoaling surface gravity waves. *Phil. Trans. R. Soc. Lond, A311*: 1-41.

Freilich, M.H., R.T. Guza and S. Elgar, 1990. Observations of nonlinear effects in directional spectra of shoaling gravity waves. *J. Geophys. Res., 95*: 9645-9656.

Luth, H.R., G. Klopman and N. Kitou, 1994. Project 13G: Kinematics of waves breaking partially on an offshore bar; LDV measurements for waves with and without a net offshore current. *Delft Hydraulics*, Report H1573, 40 pp.

Madsen, P.A., R. Murray, and O.R. Sørensen, 1991. A new form of the Boussinesq equations with improved linear dispersion characteristics. *Coastal Eng., 15*: 371-388.

Madsen, P.A. and O.R. Sørensen, 1992. A new form of the Boussinesq equations with improved linear dispersion characteristics. Part 2: A slowly-varying bathymetry. *Coastal Eng., 18*: 183-204.

Madsen, P.A. and O.R. Sørensen, 1993. Bound waves and triad interactions in shallow water. *Ocean Eng., 20(4)*: 359-388.

Nwogu, O., 1993. An alternative form of the Boussinesq equations for modelling the propagation of waves from deep to shallow water. *J. of Waterway, Port, Coastal and Ocean Eng., 119(6)*: 618-638.

Peregrine, D.H., 1967. Long waves on a beach. *J. Fluid Mech., 27(4)*: 815-827.

Quinn, P.A., M. Petti, M. Drago and C.A. Greated, 1994. Velocity field measurements and theoretical comparisons for non-linear waves on mild slopes. *Mast-G8M Workshop*, Sept. 1994.

Roelvink, J.A. and A.J.H.M. Reniers, 1995. LIP 11D Delta Flume experiments. *Delft Hydraulics*, Report H2130.

Roelvink, J.A. and M.J.F. Stive, 1989. Bar-generating cross-shore flow mechanisms on a beach. *J. Geophys. Res., 94(C4)*: 4785-4800.

Schäffer, H.A., P.A. Madsen and R. Deigaard, 1993. A Boussinesq model for waves breaking in shallow water. *Coastal Eng., 20*: 185-202.

Schröter, A., 1995. Nichtlineare zeitdiskrete Seegangssimulation im flachen und tieferen Wasser. *Institut für Strömungsmechanik und Elektron. Rechnen im Bauwesen, Universität Hannover*, Bericht Nr. 42/1995.

Thornton, E.B. and R.T. Guza, 1983. Transformation of wave height distribution. *J. Geophys. Res., 88(C10)*: 5925-5938.

Witting, J.M., 1984. A unified model for the evolution of nonlinear water waves. *J. Comp. Phys., 56*: 203-236.